

# The Effect of Turbulence on Flow of Natural Gas Through Porous Reservoirs

M. R. TEK  
MEMBER AIME  
K. H. COATS\*  
JUNIOR MEMBER AIME  
D. L. KATZ  
MEMBER AIME

U. OF MICHIGAN  
ANN ARBOR, MICH.

## ABSTRACT

*The nature and the limits of validity of Darcy's law as applied to the flow of natural gas through reservoirs has been considered in order to resolve some controversial aspects of the effect of turbulence on pressure drops.*

*The equivalence between various concepts and viewpoints advanced in the past by several investigators to explain how and why a gas well does not necessarily perform according to Darcy's law is shown.*

*Starting with generalized equations of flow of fluids through porous media, a partial differential equation has been derived which accurately represents the flow at all rates. This equation has been numerically solved using an IBM 704 digital computer.*

*The results permit plots of unsteady radial pressure distribution curves from which specific isochronal back-pressure curves may be constructed. These back-pressure curves show the effect of the  $\beta$  factor on the slope of the back-pressure curve.*

*The calculations further indicate that the drainage radius for a gas well in turbulent flow propagates at a rate dependent upon the rate of production at the wellbore. This is quite different from the case with liquid flow or natural-gas flow in laminar regime.*

*Additionally, the effect of reservoir inhomogeneities and crossflow between layers of different permeability on the back-pressure performance of gas wells has been considered.*

*In light of the current numerical results the significance and limitation of the rate of flow function  $Y$  proposed by Smith<sup>1</sup> has been discussed.*

## INTRODUCTION

The relationship between the pressure drop and flow rate in problems of fluid flow through porous media is known to be affected by the nature of flow through the porous matrix. It has been observed by many that, for a range of flow rates, the pressure drop remains proportional to the rate of flow. When some flow rate is reached, however, it is usually observed that the pressure drop gradually begins to increase more than proportionally to the

flow rate. It is well known that this phenomenon was first observed by Osborne Reynolds in 1901 in experimenting with flow through pipes. In his classical experiments, Reynolds made visual observations on the condition of streamlines evidenced by injecting a dye into water flowing through glass tubes. In these experiments, the abrupt transition between steady, "streamline, laminar" flow and unsteady random turbulent flow was found to be a function of the dimensionless group  $(Dv\rho/\mu)$ , now known as the Reynolds number. During these experiments, in addition to observations on the nature of flow regimes, the proportionality between flow rate and pressure drop in laminar flow was contrasted with the nonlinearity between these variables in turbulent flow.

Fancher and Lewis<sup>2</sup> reported data on various consolidated and unconsolidated sands in 1933. Their conclusions were that ". . . the flow of fluids through these porous materials closely resembles that through pipes; that there is a condition of flow in porous systems which resembles viscous flow, another which corresponds to turbulent; that the change from one type to the other takes place at a definite and reproducible condition for each system".

In 1947, Brownell and Katz<sup>3</sup> published a method to predict the laminar and turbulent flow behavior from the particle size, bed porosity and the particle sphericity, employing the friction factor-Reynolds number charts for pipes. Several investigators have verified the work of Fancher, Lewis and Barnes and presented their data as friction factor-vs-Reynolds number plots.<sup>4</sup>

The equation which would represent the pressure gradient over the whole range of velocity must have an added term over that represented by Darcy's law. Accordingly, the pressure gradient necessary to sustain flow at the velocity ( $v$ ) through a porous medium may be represented by the following equation, suggested by Forcheimer.<sup>4</sup>

$$-\frac{dP}{dL} = \mu \frac{v}{k} + av^2 \dots \dots \dots (1)$$

The nature and the range of validity of Darcy's law has been the subject of studies by many investigators over the past years. While everyone seemed to agree on the need for a quadratic correction term to Darcy's law to make it effective over the range of velocities, the concept of inception of turbulence and the use of the term "turbulent flow" remained controversial.

Some fluid dynamicists define turbulence as a flow

Original manuscript received in Society of Petroleum Engineers office Aug. 7, 1961. Revised manuscript received June 8, 1962. Paper presented at 36th Annual Fall Meeting of SPE, Oct. 8-11, 1961, in Dallas.

\*Presently associated with Jersey Production Research Co., Tulsa, Okla.

<sup>2</sup>References given at end of paper.

regime where random fluctuations occur with time in the magnitude of velocity components. Because of the scale and geometries inherently found in consolidated porous media, the afore-mentioned concepts of turbulent flow field have been held by many to be incompatible with conditions encountered in porous matrices. With large-enough particles and pore sizes, on the other hand, it must be clear that abrupt transition from streamline flow to turbulent eddies takes place and has been observed by one of the authors.

In an article on the flow of gases through porous metals, Green and Duwez<sup>2</sup> conclude that the onset of turbulence within the pores appears unsatisfactory to explain deviations from Darcy's law. Cornell and Katz<sup>3</sup> reported measurements on porous solids and introduced a "turbulence factor" as the characteristic of the medium. In a series of articles,<sup>7</sup> Houpeurt showed that deviations from Darcy's law may be explained on the basis of kinetic energy variations and the jetting of the fluid through orifice-like interpore passages.

Schneebeli<sup>11</sup> reported that some experiments of Lindquist demonstrate that the onset of turbulence does not necessarily coincide with conditions of deviation from Darcy's law. This view is also held by Hubbert.<sup>12</sup> A generalized dimensionless form of the Darcy equation based on Houpeurt's concepts has been published by Tek.<sup>9</sup>

Recently, a correlation between a parameter  $\lambda$  (called Darcy number) and the Reynolds number has been presented for consolidated and unconsolidated porous media by Abdulvagabov.<sup>13</sup> This paper shows that, for Reynolds numbers above 20, a family of curves was found which approaches asymptotically the straight line  $\lambda = \text{constant}$ , characterizing the quadratic law of resistance to flow. This author also concludes that a special coefficient characteristic of the solid is required to fully describe the flow at high velocities.

## COMPARISON BETWEEN VARIOUS TURBULENCE FACTORS

### CONCEPT OF TURBULENCE FACTOR $\beta$

Katz and Cornell<sup>3</sup> developed Eq. 1 with the constant (a) represented by the product of the fluid density ( $\rho$ ) and a turbulence factor ( $\beta$ ) characteristic of the solid.

$$-\frac{dP}{dL} = \frac{\mu}{k} v + \beta \rho v^2 \quad (2)$$

For gases, it is more convenient to express the pressure gradient in terms of the mass velocity  $W/A = \rho v$ , because the mass velocity remains constant in a steady-state flow and a given cross-sectional area even though the gas may be expanding. Accordingly,

$$\rho \left( -\frac{dP}{dL} \right) = \rho v \frac{\mu}{k} + \beta \rho^2 v^2$$

$$= \frac{\mu W}{kA} + \beta \left( \frac{W}{A} \right)^2 \quad (3)$$

Since

$$\rho = \frac{MP}{ZRT} \quad (4)$$

then

$$-\frac{M}{RT} p_r^2 \int_{p_{r,1}}^{p_{r,2}} \frac{p_r}{Z} dp_r = \left[ \frac{\mu W}{kA} + \beta \left( \frac{W}{A} \right)^2 \right] \int_1^2 dL \quad (5)$$

$$-\frac{M}{RT} p_r^2 \left[ \int_{0.2}^{p_{r,2}} \frac{p_r}{Z} dp_r - \int_{0.2}^{p_{r,1}} \frac{p_r}{Z} dp_r \right] = \left[ \frac{\mu W}{kA} + \beta \left( \frac{W}{A} \right)^2 \right] L \quad (6)$$

The values of integrals  $\int_{0.2}^{p_r} \frac{p_r}{Z} dp_r$ ,

published by Nisle and Poettmann,<sup>14</sup> are tabulated also in Ref. 5.

When the pressure drop between Points 1 and 2 is not high, an average value of the compressibility factor may be used and the following equation may be derived.

$$\frac{M(p_1^2 - p_2^2)}{2ZRT\mu L(W/A)} = \frac{W\beta}{A\mu} + \frac{1}{k} \quad (7)$$

Flow data for a core specimen plotted in accordance with this equation is shown in Fig. 1. It can be seen from this figure and Eq. 7 that the intercept of the resulting straight line is  $1/k$  and the slope is the turbulence factor  $\beta$ . Cornell and Katz<sup>3</sup> correlated  $\beta$  with an electrical resistivity factor related to the deviation of the flow path from a straight line and a constant  $k_2$  of the porous medium. These data have been recorelated by Janicek and Katz,<sup>15</sup> resulting in the plot of Fig. 2. By observing that the resistivity factor approximates  $4/\phi$  and that  $k_2$  is related to porosity and permeability;

$$\beta = \frac{5.5 \times 10^7}{k^{0.74} \phi^{0.74}}$$

the basis for the constant porosity lines on Fig. 2.

### CONCEPT OF LITHOLOGY FACTOR $l_f$

A generalized Darcy equation in the form of friction factor-Reynolds number correlation was developed and published by Tek<sup>9</sup> in the following form.

$$f = \frac{d^5}{2kR_c} \left( 1 + l_f \frac{R_c}{\phi} \right) \quad (8)$$

where  $l_f$  = a dimensionless factor representing the particular porous medium called the "lithology factor".

The friction factor  $f$  in the preceding was defined by

$$f = -\frac{\Delta P}{\rho} \frac{d}{2Lv^3} \quad (9)$$

In combining Eqs. 8 and 9, one may write

$$-\frac{dP}{dL} = \mu \frac{v}{k} + l_f \frac{d\rho}{\phi k} v^3 \quad (10)$$

### HOUPEURT'S FLOW FACTOR

Janicek and Katz<sup>15</sup> showed that Houpeurt's factor for handling high-velocity flow was related to the turbulence

factor  $\beta$  as follows:  $\beta = \frac{\xi}{8k}$ .

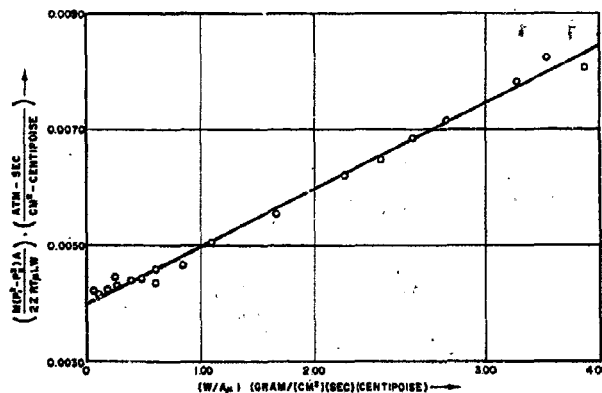


FIG. 1—EVALUATION OF PERMEABILITY  $k$  AND TURBULENCE FACTOR  $\beta$  FOR A WILCOX SAND.<sup>25</sup>

**TURBULENT FLOW—DARCY FLOW—NON-DARCY FLOW**

While turbulence has been observed for fluids flowing through porous media having passages large enough to permit visual observations, consolidated porous solids with very small particles, pores and low permeability do not permit visualization of turbulent eddies. Various explanations have been offered to explain the pressure flow behavior with high fluid velocities.<sup>8-11</sup>

Fluid particles passing through a porous bed are subject to accelerations and decelerations as they pass through constrictions and enlargements alternately. In laminar or viscous flow, characterized by Darcy's law, the kinetic energy of the particle is reversibly interchanged with the pressure energy during the acceleration and deceleration processes. At the velocity where pressure drop becomes more than proportional to the velocity, this interchange includes significant irreversibilities. What is the nature of the irreversibilities? They can only be due to extra fluid motion consuming energy, i.e., extra motion above that occurring in the laminar flow path. Some investigators refer to this phenomenon as kinetic effects, and the authors agree that the extra fluid motion is caused primarily by the inertial effects in the deceleration process, and quite likely in the absence of turbulent eddies. This phenomenon has been referred to by some investigators as "non-Darcy" flow. If one assigns the extra motion of the fluid as the cause of the extra pressure loss, then the term "turbulent flow" is justified because, in true turbulent flow in pipes, it is the extra consumption of energy which is significant to the engineer. Hence, many investigators in the field use the term "turbulent flow" simply to designate a condition of velocity such that increases in pressure drop for liquids or difference of squares of pressures for gases are more than proportional to increases in flow rates. That is the procedure followed here.

**EFFECT OF TURBULENCE IN RADIAL STEADY-STATE FLOW THROUGH GAS RESERVOIRS**

Elenbaas and Katz<sup>3</sup> using the friction factor-vs-Reynolds number plots developed by Brownell and Katz<sup>1</sup> showed

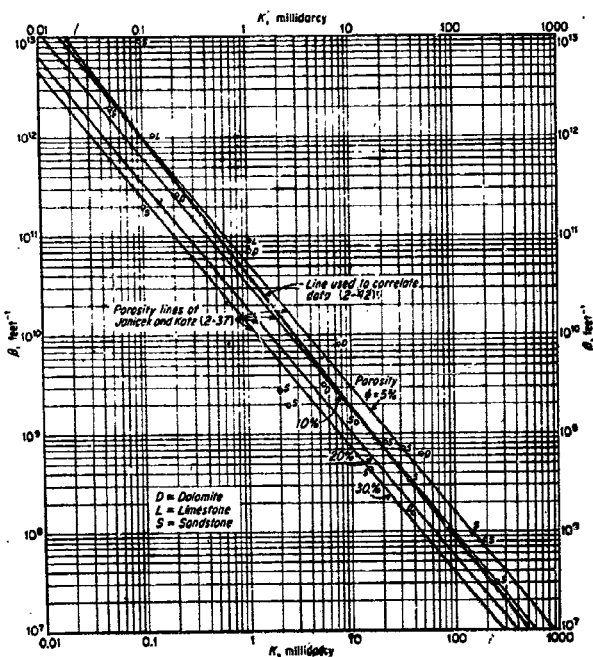


FIG. 2—CORRELATION OF TURBULENCE FACTOR  $\beta$  WITH PERMEABILITY.<sup>12</sup>

in 1948 that by graphical integration of the general flow equation through porous media one can develop a back-pressure curve relating  $(p_i^2 - p_w^2)$  to  $q$ , for a given gas well. Their results clearly show the deviation of the slope of the back-pressure curve at high flow rates from unit slope corresponding to Darcy flow regime.

For radial steady-state flow when the generalized flow equation (Eq. 2) is integrated, the following radial turbulent gas-flow equation may be derived with field units.

$$p_i^2 - p_w^2 = 1,424 \frac{\mu Z T q_g}{h k} \ln \left( \frac{r_2}{r_1} \right) + \frac{3.161 \times 10^{-13} \beta G q_g^2 Z T}{h^2} \left( \frac{1}{r_2} - \frac{1}{r_1} \right) \quad (11)$$

Using Eq. 11, back-pressure curves were computed for a 0.6-gravity gas and a temperature depth-pressure relationship for determining properties of the gas.<sup>12</sup> Permeability and initial reservoir pressure (and, hence, temperature) are parameters on the chart of Fig. 3. This chart directly relates the back-pressure curve to formation permeability.

**EFFECT OF RESERVOIR INHOMOGENEITIES ON SLOPE OF BACK-PRESSURE CURVE**

It is recognized that the steepness of the back-pressure curves on Fig. 3 is less than that found in actual cases. Accordingly, turbulence may be an insufficient explanation for the high values of the slope  $(1/n)$  sometimes found for gas wells. The question arises as to whether inhomogeneities could cause steeper curves. Calculations are made for a given millidarcy-foot product, assuming first homogeneous sand and then layered sand of different permeabilities.

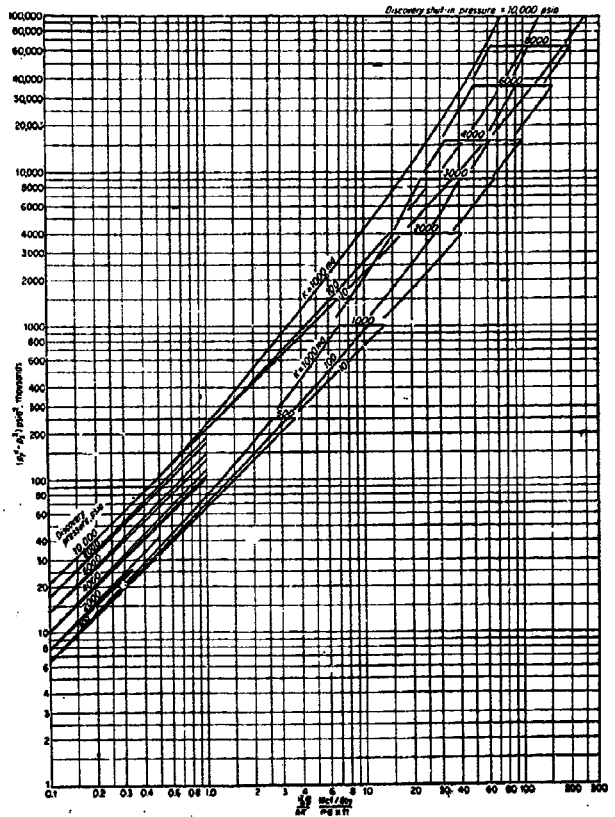


FIG. 3—PERFORMANCE CURVES FROM CORE DATA FOR 0.6-GRAVITY GAS.<sup>12</sup>

Consider a back-pressure curve calculated from Eq. 11 for a gas well and reservoir having the following properties:  $r_w = 1/3$  ft,  $M = .6(29) = 17.4$ ,  $\mu = .0125$  cp,  $T = 540^\circ\text{R}$ ,  $p_s = 14.7$  psia,  $\phi = 0.18$ ,  $r_1 = 1,320$  ft (160-acre spacing), and  $z = .92$ . Insertion of these data into Eq. 11 yields

$$p_i^2 - p_w^2 = 73 \times 10^4 \frac{q_v}{kh} + 2.82 \times 10^{-3} \frac{q_v^2 \beta}{h^2} \quad (12)$$

In these calculations  $q_v$  is given in million cubic feet. Two cases are considered. In Case I,  $kh$  is 10,000 md-ft and the reservoir is considered homogeneous, with  $k = 100$  md,  $h = 100$  ft. Thus Eq. 12 becomes

$$p_i^2 - p_w^2 = 7,300 q_v + 17.6 q_v^2 \quad (13)$$

where  $\beta = 6.2 \times 10^3$  from Fig. 2 for  $k = 100$ ,  $\phi = .18$ . Eq. 13 is plotted in Fig. 4. The reciprocal slope of the back-pressure curve is shown on Fig. 4 to be close to 1.0 at low rates of flow, and significantly less than 1.0 (.874) at higher rates. For the case  $\beta = 0$ , of course, the slope would be 1.0 for all rates.

In Case II,  $kh$  is again taken as 10,000 md-ft, but the reservoir is considered stratified into a zone 8-ft thick with  $k = 1,000$  md, and a zone 92-ft thick with  $k = 21.7$  md. If the pressure distribution in the reservoir during production were truly steady-state, then no crossflow would exist between the layers and Eq. 12 could be applied separately to each layer. Although such a steady state may not be actually attained, it will be assumed in order to gain an indication of the effect of stratification on back-pressure curves. For the 8-ft zone,  $\beta = 4 \times 10^3$  1/ft for  $k = 1,000$  md and  $\phi = .18$  (from Fig. 2), and Eq. 12 becomes

$$p_i^2 - p_w^2 = 9,140 q_v + 177 q_v^2 \quad (14)$$

For the 92-ft zone,  $\beta = 4.5 \times 10^3$  for  $k = 21.7$  md and Eq. 12 becomes

$$p_i^2 - p_w^2 = 36,500 q_v + 149 q_v^2 \quad (15)$$

For a given value of  $(p_i^2 - p_w^2)$ , the production rate from the 8-ft zone is calculated from Eq. 14, that for the

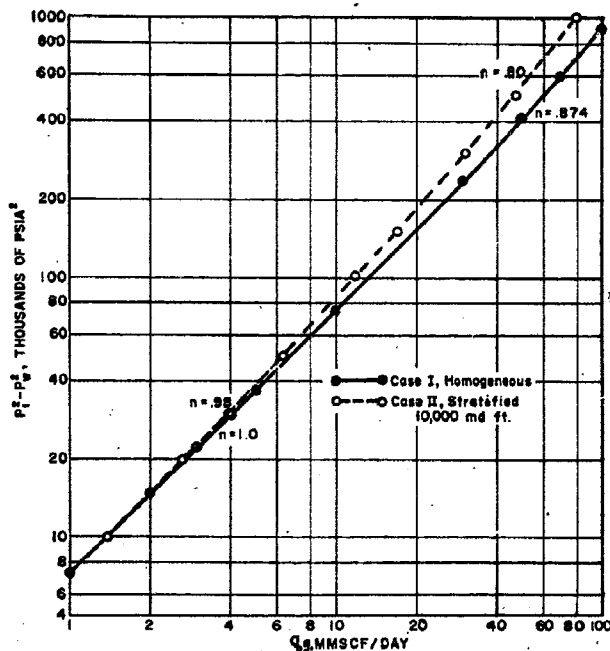


FIG. 4—EFFECT OF TURBULENCE AND STRATIFICATION ON RECIPROCAL SLOPE OF BACK-PRESSURE CURVE.

92-ft zone is calculated from Eq. 15 and these two rates are added together to give the total production rate. This total rate  $q_v$  is plotted in Fig. 4 as "Case II".

The reciprocal slope of the back-pressure curve for Case II is again seen to be nearly 1.0 at low rates, and significantly lower than 1.0 at higher rates. At rates of 30 to 80 MMcf/D, the reciprocal slope of the stratified reservoir is seen to be .80 as compared with .874 for the homogeneous formation. Thus while turbulence, as represented by the  $\beta$  factor, lowers the reciprocal slope, stratification can be an added factor tending to decrease it further. A more severe degree of stratification or fracturing would tend to increase the difference in reciprocal slopes of the two curves at high flow rates. Since gas production involves unsteady-state flow to a degree, crossflow occurs in stratified systems and such crossflow is likely to magnify the effect of turbulence on the slope of the back-pressure curve.

#### UNSTEADY-STATE FLOW OF GAS INCLUDING EFFECTS OF TURBULENCE

The treatments of unsteady-state gas flow have been presented using Darcy's law to represent the flow relationships.<sup>17,18</sup> The unsteady-state calculations have been necessary to understand the behavior of tight formations. The isochronal procedure<sup>19</sup> is based on the concept of equal radii of drainage at equal flow times. The unsteady-state flow relationships have been used to determine in situ formation properties from well data. Smith<sup>20</sup> used a "rate-of-flow function" empirically to correct a correlation<sup>18</sup> involving only Darcy's law. In this paper, unsteady-state flow is calculated with the generalized flow equation including the turbulence factor.

#### DERIVATION OF EQUATIONS

When the generalized relationship of Eq. 2 between the pressure gradient and the superficial velocity is combined with the continuity equation and the equation of state for natural gas, the following equations result.

$$\frac{\partial P^2}{\partial r_D} = q_D \frac{1}{r_D} + B \frac{q_D^2}{r_D^2} \quad (16)$$

and

$$\frac{1}{r_D} \frac{\partial q_D}{\partial r_D} = \frac{1}{P} \frac{\partial P^2}{\partial t_D} \quad (17)$$

where  $q_D = 50.2 \times 10^3 q_v \mu P_s T_z / h k p_i^2 T_w$ , dimensionless flow rate in field units,

$P = p/p_s$ , dimensionless pressure,

$r_D = r/r_w$ , dimensionless radius, and

$t_D = 2.634 \times 10^{-4} \frac{k p_i t}{\mu \phi r_w^2}$ , dimensionless time.

In deriving Eqs. 16 and 17, a horizontal disk-shaped porous medium of constant thickness is assumed. The viscosity of the natural gas and the compressibility factor  $Z$  are also assumed to be constant.

In Eq. 16,

$$B = 5.37 \times 10^{-8} \frac{\beta M k^2 p_i^2}{T Z \mu^2 r_w} \quad (18)$$

Eqs. 15 and 17 are two simultaneous partial differential equations in the dependent variables  $\bar{Q}$  and  $P$ , which must be solved along with the following boundary conditions.

$$q_D = q_{D0} \text{ at } r_D = 1.0, t_D \geq 0 \quad (19)$$

$$q_D = 0 \text{ at } r_D = \frac{r_e}{r_w}, t_D \geq 0 \quad (20)$$

The equations and the boundary conditions, Eqs. 16 through 20, are for constant terminal rate for a radial

flow model with closed exterior boundary. Initially,  $P^2$  is equal to unity throughout the reservoir and  $q_D = 0$ .

A solution to Eqs. 16 and 17 may be obtained by using the transformation  $x = \ln r_D$ .

$$\frac{\partial P^2}{\partial x} = q_D + B e^{-x} q_D^2 \quad (21)$$

$$\frac{\partial q_D}{\partial x} = \frac{e^{-2x}}{P} \frac{\partial P^2}{\partial x} \quad (22)$$

This transformation permits closely spaced radial increments near the wellbore, corresponding to equally spaced increments in  $x$ . Solving for  $\frac{\partial q_D}{\partial x}$  from Eq. 21, and substituting in the Eq. 22, yields

$$\left( \frac{P e^{-2x}}{1 + 2B e^{-x} q_D} \right) \frac{\partial P^2}{\partial x^2} + \frac{B P e^{-2x} q_D^2}{1 + 2B e^{-x} q_D} = \frac{\partial P^2}{\partial t_D} \quad (23)$$

or

$$C \frac{\partial^2 P^2}{\partial x^2} + D = \frac{\partial P^2}{\partial t_D} \quad (24)$$

Eq. 24 may be replaced by the following implicit finite-difference form.

$$C_{m,n+1}^{(i)} P_{m,n+1}^{z^{(i+1)}} - \left( 2C_{m,n+1}^{(i)} + \frac{\Delta x^2}{\Delta t_D} \right) P_{m,n+1}^{z^{(i+1)}} + C_{m,n+1}^{(i)} P_{m-1,n+1}^{z^{(i+1)}} = -\Delta x^2 D_{m,n+1}^{(i)} - \frac{\Delta x^2}{\Delta t_D} P_{m,n}^{z^{(i)}} \quad (25)$$

where  $x = m\Delta x$ ,

$t_D = n\Delta t_D$ , and

$i$  = the index of iteration.

The coefficients  $C$  and  $D$  are evaluated at the new time step but at the previous iteration ( $i$ ). Eq. 25, when written for  $m = 1, 2, \dots, M$ , (where  $M\Delta x = x_e = \ln r_e/r_w$ ), constitutes a tridiagonal matrix which is solved by a method given by Richtmyer.<sup>18</sup> Eq. 21 is solved for each time step recalculating the coefficients  $C$  and  $D$  at each new iteration until the maximum change in  $P^2$ ,

$$\text{Max} \left| P_{m,n+1}^{z^{(i+1)}} - P_{m,n+1}^{z^{(i)}} \right|,$$

is less than a prescribed tolerance  $\epsilon$ .

The calculations were programmed for and performed on an IBM 704 computer. The case of a finite reservoir with a ratio  $r_e/r_w = 128$  was treated; the boundary conditions at  $r_e$  and  $r_w$  were obtained by simply inserting  $q_D = 0$  and  $q_D = q_{D0}$ , respectively, into Eq. 21. The dimensionless time increment  $\Delta t_D$  was increased from 0.001 early in the calculations to 10 when  $t_D$  exceeded 120. Twenty-five spatial increments and a tolerance of  $5 \times 10^{-3}$  were employed in the calculations.

### DISCUSSIONS OF RESULTS

Fig. 5 represents a typical set of isochronal back-pressure curves obtained for a given value of  $B$  coefficient and for several values of dimensionless time  $t_D$ . The curves in Fig. 5 are for the generalized case where the effect of turbulence factor has been included in the unsteady state. The partial differential equations have been solved numerically without resorting to any linearization technique. For the sake of simplicity, however, the  $z$  factor has been treated as a constant evaluated at static reservoir conditions. The parallel trend and gradual shifting of the curves to the left as time goes on are noted.

A typical set of back-pressure curves indicating the effect of  $\beta$  factor on the slope is illustrated in Figs. 6 and

7. It may be noted, as expected, that the increase in  $B$  results in increased reciprocal slopes for a given flow rate and given value of time.

Eq. 2 gives the pressure gradient  $\left( -\frac{dp}{dr} \right)$  as a function of velocity including the turbulent contribution  $\beta \rho v^2$ . Integration of this equation between  $r_w$  where  $p = p_w$  and  $r_1$  where  $p = p_1$  yields

$$\left( \frac{p_1/p_r}{r_w} - \frac{1}{r_1} \right) = q_D \ln \frac{r_1}{r_w} + \frac{q_D^2 \beta M k^2 p_r^2}{2R\mu TZ} \quad (26)$$

Eq. 26 is valid for steady-state gas flow between a point in the reservoir radius  $r_1$  and the wellbore radius  $r_w$ . The term  $q_D$  is a dimensionless production rate and  $p_r$  is shut-in reservoir pressure at the time when production is begun.

Aronofsky and Jenkins<sup>19</sup> replaced  $r_1, p_1$  in Eq. 26 by  $r_e, p_e$ , dropped the term containing  $q_D^2$ , and used the resulting equation

$$\ln \frac{r_e}{r_w} + \frac{1}{q_D} [(p_e/p_r)^2 - (p_w/p_r)^2] \quad (27)$$

to define a "drainage radius"  $r_e$ . The pressure  $p_e$  is the pressure the reservoir would attain if it were shut in and allowed to equalize. As gas is produced,  $p_e$  will thus decrease; use of a material balance yields Eq. 18.

$$p_e/p_r = 1 - q_D \theta \quad (28)$$

where  $\theta = 2.634 \times 10^{-4} k p_r t / \mu \phi r_e^2$ , a dimensionless time.

Thus, Eq. 27 becomes

$$\ln \frac{r_e}{r_w} = \frac{1}{q_D} [(1 - q_D \theta)^2 - (p_w/p_r)^2] \quad (29)$$

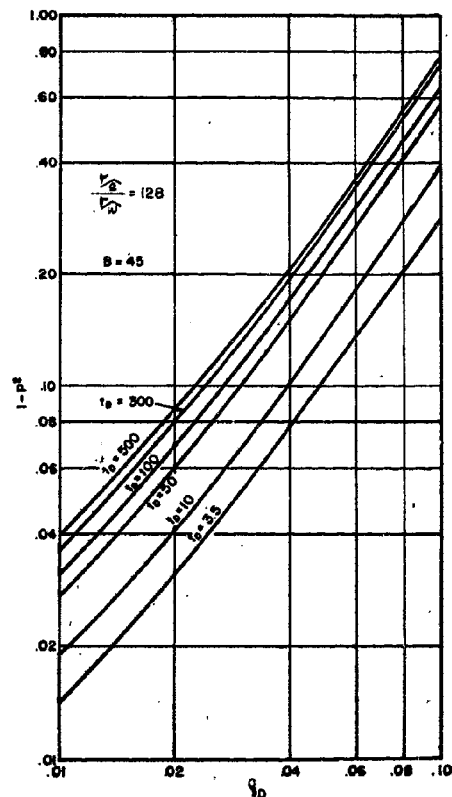


FIG. 5—COMPUTED ISOCHRONAL BACK-PRESSURE CURVES FOR A GAS RESERVOIR.

Aronofsky and Jenkins<sup>11</sup> numerically solved the unsteady-state gas-flow equation derived from Darcy's law,

$$\frac{\partial^2 p^2}{\partial r^2} + \frac{1}{r} \frac{\partial p^2}{\partial r} = \frac{2 \phi \mu}{k} \frac{\partial p}{\partial t} \quad (30)$$

and inserted the solution in terms of  $q_D$  and  $p_w$  into the right-hand side of Eq. 29. Their result was that  $\ln r_s/r_w$  was closely given by the equation

$$\ln \frac{r_s}{r_w} = p_i - 2t_D \left( \frac{r_w}{r_s} \right)^2 = p_i - 2\theta \quad (31)$$

Smith,<sup>12</sup> in an attempt to account for deviations from Darcy flow, modified Eq. 29 to read

$$Y_q + \ln \frac{r_s}{r_w} = \frac{1}{q_D} [(1 - q_D \theta)^2 - (p_w/p_i)^2] \quad (32)$$

where  $Y_q$  was claimed to be a dimensionless function of flow rate, and the assumption was made that  $\ln \frac{r_s}{r_w}$  is still given by Eq. 31.

In the preceding section, equations are developed which govern unsteady-state gas flow when turbulence is taken into account. These equations have been solved numerically to obtain the relationship between  $q_D$ ,  $p_w$  and  $\theta$  which appear in the right-hand side of Eq. 29. Insertion of these calculated quantities into Eq. 29 then gives  $\ln (r_s/r_w)$  as a function of time.

In Figs. 8 and 9,  $\ln (r_s/r_w)$  is plotted vs time with  $B$  and  $q_D$  as parameters. These figures show that  $\ln (r_s/r_w)$ , as defined by Eq. 29, depends upon  $q_D$  when turbulence or non-Darcy flow is taken into account. Since Smith substituted  $\ln (r_s/r_w)$  from Eq. 31 into Eq. 32, his  $Y(q)$  function must account for or absorb the differences in time-dependency of  $\ln r_s/r_w$  shown in Figs. 8 and 9. These figures also show that the curve of  $\ln (r_s/r_w)$  vs

time is shifted by or dependent upon the factor  $B$ . Thus, the  $Y(q)$  function should be denoted as  $Y(q, t_D, B)$ , since all three of these variables affect  $Y$ . It should be noted that, where isochronal testing is employed and a single well is involved,  $t_D$  and  $B$  are fixed and  $Y$  reduces to a function of flow rate only. However, the values of  $Y(q)$  calculated as described by Smith will depend upon the time duration of the isochronal test provided stabilization has not occurred. At stabilization,  $\ln (r_s/r_w)$ , and therefore  $Y$ , ceases to be time-dependent, as shown in Figs. 8 and 9.

### NOMENCLATURE

- $A$  = cross-sectional area to flow, sq cm
- $a$  = a constant for a given porous medium, lb mass/ft<sup>4</sup>
- $B$  = a constant ( $B = 5.37 \times 10^{-20} \beta M k^2 p_i^2 / T z \mu^2 r_w$ )
- $C$  = constant function of  $q^2$  flow rate and pressure, dimensionless
- $D$  = constant function of flow rate and pressure, dimensionless; also, diameter in Reynolds number
- $d$  = mean particle diameter, ft
- $d()$  = denotes total differentiation
- $f$  = friction factor, dimensionless
- $G$  = gas gravity, dimensionless
- $k$  = permeability, md
- $L$  = length of the flow path, ft
- $l_i$  = lithology factor
- $M$  = molecular weight of the gas, lb/lb mole
- $p$  = pressure, psia
- $P$  = dimensionless pressure

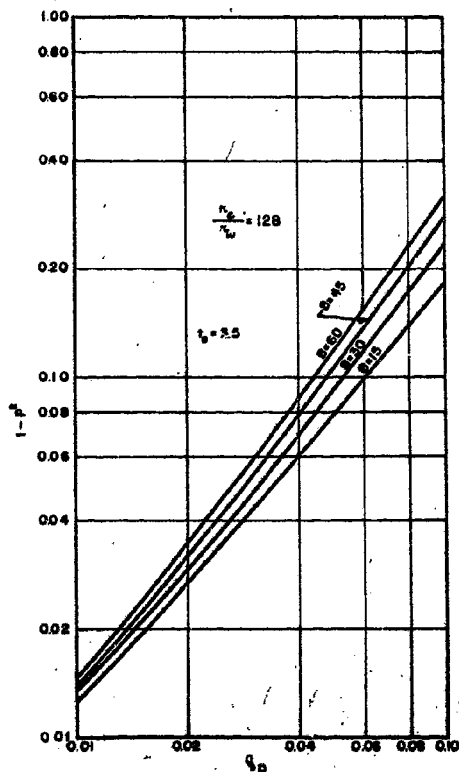


FIG. 6—EFFECT OF TURBULENCE ON ISOCHRONAL BACK-PRESSURE CURVES,  $t_D = 3.5$ .

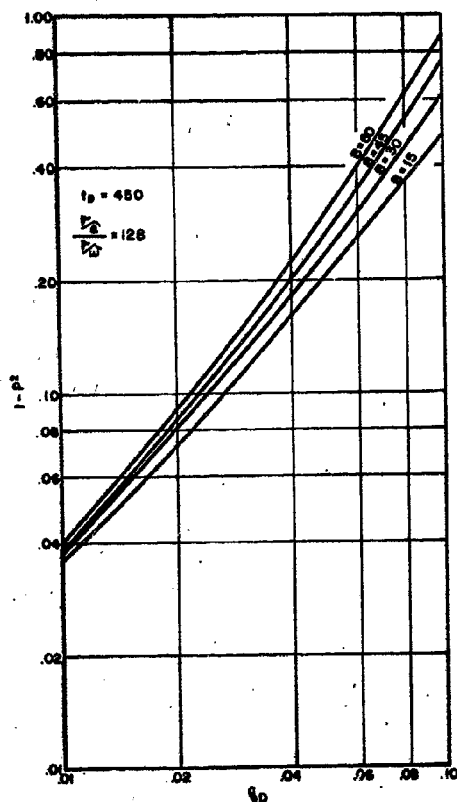


FIG. 7—EFFECT OF TURBULENCE ON ISOCHRONAL BACK-PRESSURE CURVES,  $t_D = 450$ .

$P_b$  = base pressure, psia  
 $p_r$  = pseudoreduced pressure  
 $p_s$  = pseudocritical pressure, psia  
 $p_i$  = initial static formation pressure, psia

$p_w$  = flowing sand-face pressure, psia  
 $p_e$  = van Everdingen-Hurst dimensionless pressure drop  
 $q_o$  = rate of production, Mcf/D

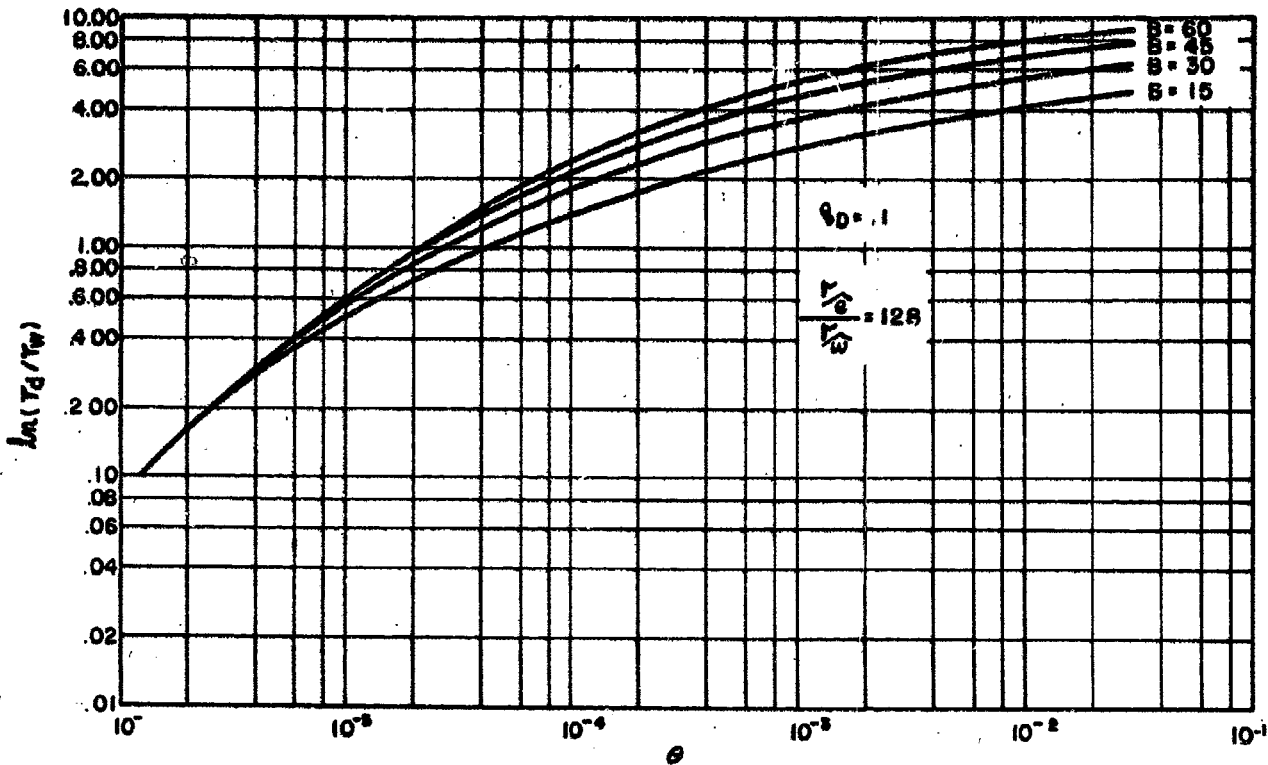


FIG. 8—EFFECTIVE DRAINAGE RADIUS VS TIME,  $q_D = 1.0$ .

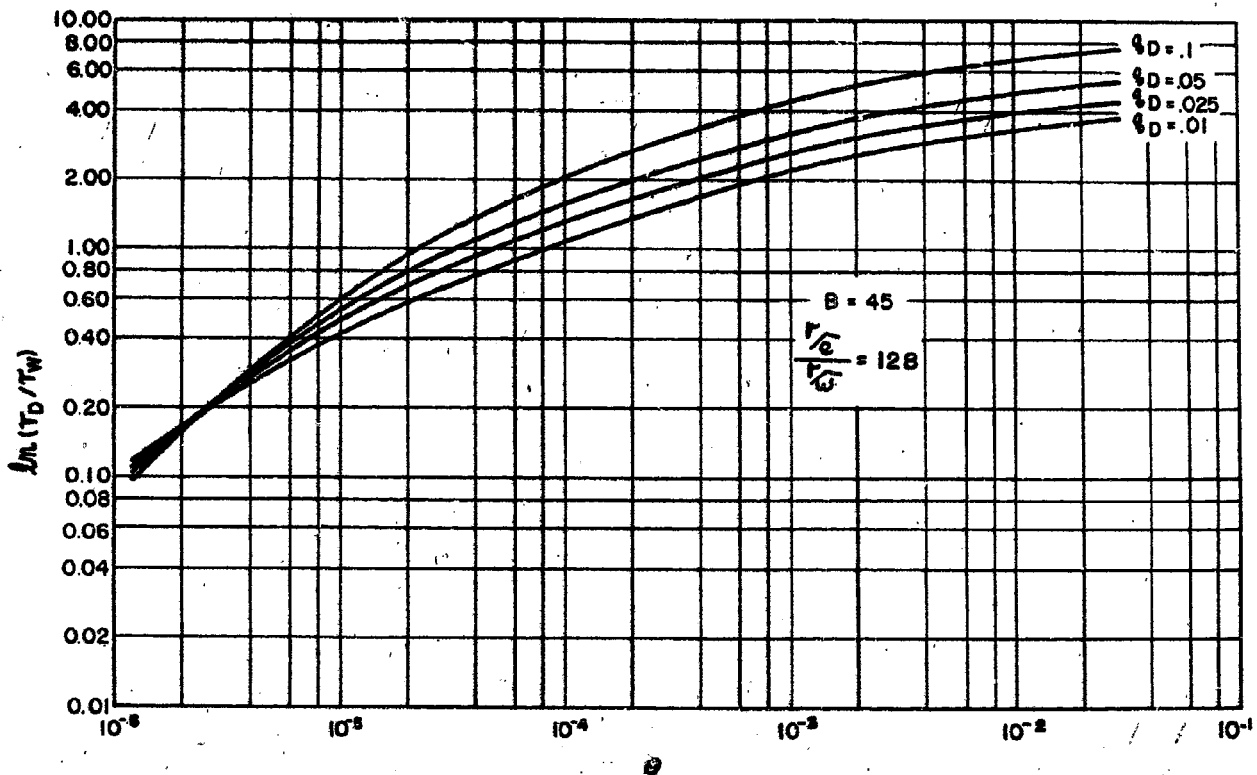


FIG. 9—EFFECTIVE DRAINAGE RADIUS VS TIME,  $B = 45$ .

$q_D$  = dimensionless flow rate  
 $R$  = gas constant,  $R = 1,544 \text{ ft} \cdot \text{lb-force/lb-mole} \cdot \text{°R absolute}$   
 $R_n$  = Reynolds number  $R_n = (\rho v D / \mu)$ , dimensionless  
 $r_w$  = well radius, ft  
 $r_e$  = radius of exterior boundary of reservoir, ft  
 $r_d$  = drainage radius, ft  
 $r_D$  = dimensionless radius,  $r/r_w$   
 $T$  = formation temperature, °R  
 $t$  = actual time, hours  
 $t_D$  = dimensionless time,  $2.634 \times 10^{-4} \frac{k p_i t}{\mu \phi r_w^2}$   
 $T_b$  = base temperature, °R absolute  
 $v$  = fluid velocity, ft/sec  
 $W$  = mass flow rate, gm/sec  
 $x$  =  $\ln r_D$   
 $Z$  = compressibility factor, dimensionless  
 $\beta$  = turbulence factor,  $\text{ft}^{-2}$   
 $\Delta$  = incremental quantity  
 $\rho$  = density of fluid, lb mass/cu ft  
 $\mu$  = gas viscosity, cp  
 $\phi$  = porosity, dimensionless  
 $\theta$  = dimensionless time,  $2.634 \times 10^{-4} \frac{k p_i t}{\mu \phi r_w^2}$   
 $\zeta$  = Houpeurt flow factor,  $\text{md} \times \text{ft}^{-1}$

#### SUBSCRIPTS — SUPERSCRIPTS

$i$  = iteration  
 $j$  = iteration  
 $0$  = initial condition  
 $1$  = upstream condition  
 $2$  = downstream condition

#### REFERENCES

1. Fancher, G. H., Lewis, J. A. and Barnes, K. B.: "Some Physical Characteristics of Oil Sands", *Bull. 12*, Pennsylvania State College Mineral Industries Experiment Station (1933) 65; also *Ind. Eng. Chem.* (1933) 25, 1139.

2. Brownell, L. E. and Katz, D. L.: "Flow of Fluids Through Porous Media" *Chem. Eng. Prog.* (1947) 43, 537.
3. Elenbaas, J. R. and Katz, D. L.: "A Radial Turbulent Flow Formula", *Trans., AIME* (1948) 174, 25.
4. Cornell, D. and Katz, D. L.: "Flow of Gases Through Porous Media", *Ind. Eng. Chem.* (1953) 45, 2145.
5. Katz, D. L., Cornell, D., Kobayashi, R., Poettmann, F. H., Vary, J. A., Elenbaas, J. R. and Weinaug, C. F.: *Handbook of Natural Gas Engineering*, McGraw-Hill Book Co., Inc., N. Y. (1959).
6. Tek, M. R.: "Development of a Generalized Darcy Equation", *Trans., AIME* (1957) 210, 376.
7. Houpeurt, A.: "Etude Analogique de L'Ecoulement Radial Circulaire Transitoire des Gas Dans les Millieux Poreux", *Revue de l'Institut Francais du Petrole et Annales des Combustibles Liquides* (1953) VIII, No. 4, 5 and 6.
8. Green, L. and Duwez, P.: "Fluid Flow Through Porous Metals", *Jour. Appl. Mech.* (1951) 18, 39.
9. Janicek, J. D. and Katz, D. L.: "Applications of Unsteady State Gas Flow Calculations", Preprint from Res. Conf., U. of Michigan, (June 20, 1955).
10. Cornell, D. and Katz, D. L.: "Pressure Gradients in Natural Gas Reservoirs", *Trans., AIME* (1953) 198, 61.
11. Schneebeli, G.: "Sur la Theorie des Ecoulements de Filtration", *La Houille Blanche* (1953) 186, No. Special A.
12. Hubbert, M. King: "Darcy's Law and the Field Equations of the Flow of Underground Fluids", *Trans., AIME* (1956) 207, 222.
13. Abdulvagabov, A. I.: *Izv. Vyss. Uch. Zaved., Nefti i Gaz*, (1961) No. 4, 83 (Russian).
14. Bakhmeteff, B. A. and Feodoroff, N. V.: "Flow Through Granular Media", *Trans., AIME* (1937) 59, A97.
15. Nisle, R. G. and Poettmann, F. H.: "Calculation of the Flow and Storage of Natural Gas in Pipe" *Pet. Eng.* (1955) 27, D14; C36; D37.
16. Richtmyer, R. D.: *Difference Methods for Initial Value Problems*, Interscience Publishers, Inc., N. Y. (1957) 103.
17. Smith, R. V.: "Unsteady State Gas Flow into Gas Wells", *Jour. Pet. Tech.* (Nov., 1961) 1151.
18. Aronofsky, J. S. and Jenkins, R. A.: "Simplified Analysis of Unsteady Radial Gas Flow", *Trans., AIME* (1954) 201, 149.
19. Cullender, M. H.: "The Isochronal Performance Method of Determining the Flow Characteristics of Gas Wells", *Trans., AIME* (1955) 204, 137.
20. Tek, M. R., Grove, M. L. and Poettmann, F. H.: "Method for Predicting the Back Pressure Behavior of Low Permeability Natural Gas Wells", *Trans. AIME* (1957) 210, 302. ★★★